

On the Resistance Prediction of High-Speed SemiSWATH hull forms

G. Zaraphonitis, G. Grigoropoulos & D. Mourkoyiannis
National Technical University of Athens, Greece

ABSTRACT: The paper focuses on the prediction of the calm water resistance of high-speed twin hull vessels of the semi-SWATH configuration. To this end, a series of model tests have been performed in the towing tank of the NTUA-LSMH. Two models of semi-SWATH hull forms have been used, sharing the same wetted length and immersed volume but with otherwise different hull forms. On the basis of the experimental results, the effects of the draft, the static trim and the spacing between the deihulls on the resistance and the interaction effects at various speeds of advance are investigated. The obtained experimental results are compared with numerical predictions that have been derived using mature potential flow solvers in an attempt to assess the capabilities of the latter to provide reliable resistance estimations. Furthermore, the model tests provide the background for the estimation of the form resistance coefficient of this type of hull forms.

1 INTRODUCTION

The prediction of the calm water resistance of high-speed twin-hull vessels has been treated by many researchers during the last twenty years. Insel and Molland (1992) and Molland et al. (1996) conducted a series of resistance tests, using a number of models derived by linear transformation of the well known NPL systematic series of round-bilge, high-speed monohull vessels. Based on the obtained results, they proposed a decomposition of the total resistance in three main components. The accurate prediction of the total resistance and of the required propulsion power of a new ship requires proper treatment of all of them and may involve detailed CFD calculations, along with extensive model testing. In the preliminary design stage, however, the availability of a fast and easy to use method for the evaluation of the performance of alternative designs would be quite useful to the designer, searching for the 'optimum' hull form under the given constraints and operational requirements. Sahoo et al. (2007) presented an overview of published work on the prediction of the resistance of twin-hull vessels along with the results of regression analysis, facilitating the calculation of the main components of the bare-hull calm water resistance.

The importance of robustness and speed of calculation of the employed procedure for the

evaluation of bare hull resistance is particularly high in the case of optimization studies, when thousands of alternative hull forms must be investigated. In this type of studies, the user is interested in finding the optimum design for a given operational scenario, and therefore his main interest is the comparison of the relative performance of one design against the others. Once the optimum design has been identified, its performance may be reevaluated with increased accuracy in a subsequent stage. Therefore, the use of potential flow theory is an obvious choice for this type of applications, due to the significant reduction of the required calculation time compared to viscous flow calculations. Empirical correction terms, derived from the analysis of experimental measurements, accounting for the viscous pressure components of the total resistance may be introduced to improve the accuracy of the results. Minor errors in the resistance calculation, resulting from this simplification may be tolerated, provided that they do not impair the correct ranking of the alternative designs, so that the optimum may still be identified.

An integrated methodology for the preliminary design and optimization of high-speed, twin-hull RoRo-Passenger vessels has been presented by Skoupas et al. (2009), developed in the context of a large research project, that has been carried out in the School of Naval Architecture and Marine

Engineering of the National Technical University of Athens. For the calculation of the calm water resistance of the alternative designs, the above-mentioned procedure relies on the use of CFD tools employing potential flow calculations to keep the required calculation time within acceptable limits. In order to evaluate the accuracy of the employed procedure and to investigate the possibility of deriving appropriate 'empirical' corrections to improve the numerical predictions, a series of tank tests has been performed in the towing tank of the Laboratory for Ship and Marine Hydrodynamics, at the National Technical University of Athens, using two models of semi-SWATH hull forms that have been specifically constructed. The details of the tank tests and the comparison of the experimental measurements with the numerical results are presented in the following.

2 RESISTANCE PREDICTION

As already mentioned, the calm water resistance of a high-speed twin-hull vessel is the sum of several components. Their number is greater than that in the case of a slow-speed displacement hull and their relative importance varies considerably with the speed of advance and the type of lift that supports the weight of the vessel. The total resistance coefficient of a monohull vessel may be expressed as follows:

$$C_T = C_F + C_R = (1+k)C_F + C_W \quad (1)$$

where:

C_T	is the total resistance coefficient
C_F	is the frictional resistance coefficient
C_R	is the residual resistance coefficient
C_W	is the wave resistance coefficient
$1+k$	is the form factor

The frictional resistance coefficient in eq. (1) is usually calculated based on the ITTC-1957 correlation line. The total resistance coefficient in model-scale may be calculated from tank tests, while the residual resistance coefficient may be subsequently calculated from eq. (1). The wave resistance coefficient may be calculated from the analysis of the measured wave pattern, or by the use of CFD tools, employing potential flow calculations. For a twin-hull vessel, Insel and Molland (1992) and Molland et al. (1996) used a variation of eq. (1) of the following form:

$$C_T = (1 + \beta k)C_F + \tau C_W \quad (2)$$

where C_W in eq. (2) refers again to the demi-hull in isolation, whereas the interference of the wave systems of the two demi-hulls is accounted for by the additional factor τ . An additional factor β is

introduced in eq. (2) to account for the interference effects on the viscous resistance. Typical form factors for high-speed displacement Catamarans have been presented in several papers, see for example Molland et al. (1996), Couser et al. (1997). The wave resistance coefficient C_W and the wave resistance interference factor τ may be derived experimentally from the wave pattern analysis, or numerically by potential flow calculations. Similar expressions with that in eq. (2) have been used by many researchers in the last ten years for the prediction of the calm water resistance of twin-hull vessels.

One of the basic aims of the present study was to provide appropriate estimations for the form factor values of semi-SWATH vessels, operating in Froude numbers between 0.6 and 0.7 with a length to volume ratio ($L/\nabla^{1/3}$) between 8.8 and 9.5, to serve as a basis for the resistance calculations within an integrated preliminary design and optimization methodology (Skoupas et al. 2009). To this end, a series of tank tests has been performed with two semi-SWATH models. In the present study, the wave resistance coefficient C_W and the wave resistance interference factor τ are derived by potential flow calculations employing the well-known CFD software SHIPFLOW (Larson, 1993). Factors β and k are subsequently calculated from eq. (1) and (2).

3 DESCRIPTION OF THE MODELS

The two hull forms that have been developed are considered typical of large modern semi-SWATH RoRo-Passenger vessels, operating at Froude numbers from 0.6 to 0.7. In order to investigate the effect of hull form on the vessel's resistance, both models have been designed with the same underwater length (including the bow bulb) of 4.0m and an immersed volume at the design draught of 0.0933m³, corresponding to a ratio of length to displacement equal to $L/\nabla^{1/3}=8.82$. With a scale of 17.5:1 they correspond to full-scale ships of 70.0m in length with an immersed volume of 1000m³ at the design draught. Their hull form is given in Figure 1 and Figure 2, while their main particulars are summarized in Table 1. Additional hydrostatic data for the two models at the three draughts for which the experiments were conducted are presented in Table 2. The length to immersed volume ratio ($L/\nabla^{1/3}$) presented in Table 2 is based on the immersed length of each model. Model A has a design draught of 0.189m and a maximum demi-hull width at the waterline of 0.229m ($B/T=1.21$), while Model B is relatively wider and more shallow, with a design draught of 0.177m and a maximum width at

waterline of 0.269m ($B/T = 1.513$). Model A has a shorter length at waterline, resulting in a much longer bulbous bow than Model B. In addition, the bulbous bow of Model A has a more 'rounded' form, while that of Model B has a comparatively 'wedge-type' shape. Finally, Model A has a round bilge shape throughout its entire length, while the hull form of Model B is designed with a chine extending for 30% of the immersed length from the transom towards the bow. It should be noted here that despite the widely acknowledged advantages of the semi-SWATH type of hull forms, most of the

published results refer to the conventional type of demi-hulls, either round bilge, or with a hard chine. Results for three semi-SWATH hull forms have been presented by Sahoo et al. (2007).

Table 1. Main Particulars of the Models

	Model A	Model B
Immersed length (L_{HL})	4.0m	4.0m
Design draught (T)	0.189	0.177m
Max. Demihull width at design WL (B_{WL})	0.229	0.269m
Transom width at design waterline	0.217m	0.269m
Transom immersion	0.075m	0.079m

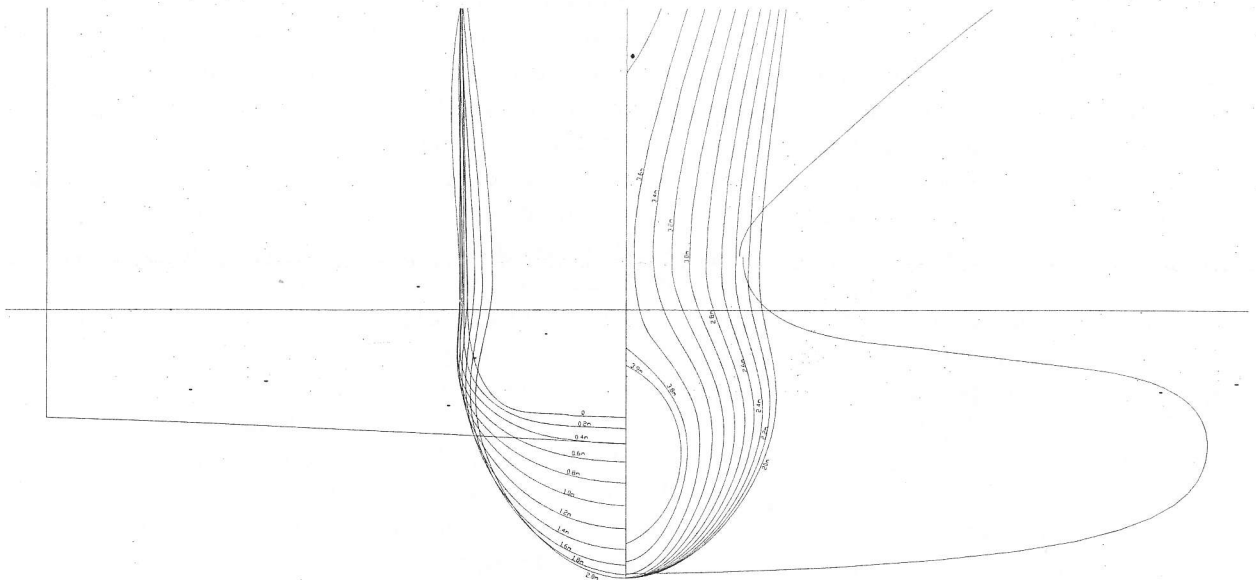


Figure 1. Hull form of Model A.

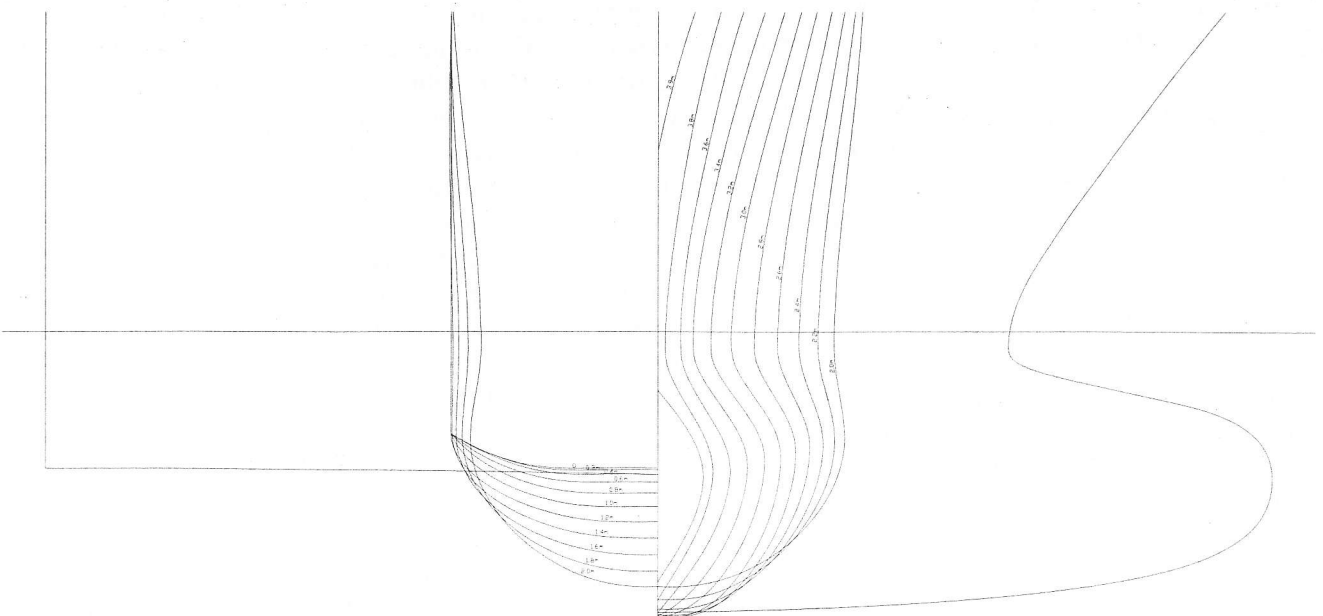


Figure 2. Hull form of Model B.

Table 2. Hydrostatic Properties of the Models (the data refer to demi-hulls)

	Model A			Model B		
	$T=0.160\text{m}$	$T=0.174\text{m}$	$T=0.189\text{m}$	$T=0.152\text{m}$	$T=0.165$	$T=0.177\text{m}$
Immersed Volume (∇) [m ³]	0.07464	0.08398	0.09322	0.07464	0.08397	0.09329
Wetted Surface [m ²]	1.4792	1.5935	1.7045	1.4922	1.5935	1.6914
Waterline Area [m ²]	0.6726	0.6491	0.6273	0.7654	0.7442	0.7350
$L/\nabla^{1/3}$	8.8194	9.1347	9.5005	8.8194	9.1347	9.5005
Length at waterline (L_{WL}) [m]	3.8177	3.7263	3.6977	3.8880	3.8417	3.8286
LCB [m]	1.9800	1.9302	1.8859	1.9210	1.8722	1.8297
VCB [m]	0.0992	0.1087	0.1139	0.0993	0.1059	0.1123
LCF [m]	1.5606	1.5074	1.4674	1.4994	1.4571	1.4389

4 EXPERIMENTAL INVESTIGATION

4.1 Experimental setup

Both models were constructed in lightweight tropical wood and tested in the towing tank of the Laboratory for Ship and Marine Hydrodynamics (LSMH) of the National technical University of Athens (NTUA). The dimensions of the towing tank are 91m (effective length), 4.56m (width), and 3.00 m (depth). The towing tank is equipped with a carriage achieving a maximum speed of 5.2m/sec. All the tests were performed in fresh water and covered a speed range corresponding to full-scale speeds of 8 to 33 knots (for a ship to model scale of 17.5:1). Throughout the test series, the water temperature was measured and recorded. During the tests, the calm water resistance, the sinkage at the point of attachment to the dynamometer, the dynamic trim and the towing speed of the model were recorded for each run.

The model was connected to the dynamometer on the carriage via a heave rod - pitch bearing assembly permitting the model to heave and pitch freely. The pitch bearing has been fitted on the bottom of each model, 8cm above its baseline and at the LCG. Thus, the dynamic C.G. rise was measured at that longitudinal location, specific for each tested loading condition.

4.2 Experimental Results

The experimental results are usually analyzed and extrapolated to full scale using either the Froude's or the Hughes method (Hughes, 1954). In both cases the ITTC 1957 friction line is used for the estimation of C_F . In this work, Froude's method was promoted to derive the residual resistance coefficient C_R by the following relation:

$$C_R = C_{TM} - C_{FM} \quad (3)$$

The coefficients C_{TM} , C_{FM} and C_{RM} are defined by the respective resistance components R_T , R_F and R_R

non-dimensionalized by the product $0.5\rho V^2 S$ and subscript "M" is used to denote the model scale. Within this analysis C_R encompasses both the wave resistance coefficient C_W as well as the viscous pressure resistance coefficient C_{VP} attributed to the modification of the pressure field by viscosity especially in the stern region. For slender hull forms C_{VP} does not exceed 10% of C_R with a tendency to approach lower values in the case of high speed catamarans (Zotti, 2005). In this analysis C_{VP} is expressed in terms of C_F to form eq. (1).

The waterline length and wetted surface at rest for each testing condition was used in the implementation of Froude's method, since at the tested speeds the respective dynamic quantities do not depart practically from the respective static ones. The C_R coefficients are depicted in Figures 4-9 for the tested conditions of Model A and in Figures 10-15 for Model B, respectively.

5 ANALYSIS OF RESULTS

Figure 3 presents a typical example of the obtained experimental and numerical results for Model B at an even keel draught of 0.165m, and a S/L ratio of 0.25, where S denotes the separation distance between the two demi-hulls (i.e. the transverse distance between their centerlines) and L (or L_{HL}) is the immersed length of the demi-hull. It should be noted that in all the results presented herein, the calculation of the Froude number is based on the total immersed length of the demi-hull including the bulbous bow (i.e. 4.0m for both models), rather than on the length of the waterline.

The total resistance coefficient C_T presented in Figure 3 has been obtained experimentally, while the frictional resistance coefficient C_F has been calculated from the ITTC-1957 correlation line and the residual resistance coefficient C_R is the difference between C_T and C_F . The wave resistance component of the twin-hull configuration expressed in the form τC_W has been calculated numerically using SHIPFLOW. Results, for $Fn > 0.38$ are also presented in tabular form in Table 3. The product βk appearing in the last column of Table 3 has been

obtained from the following equation, derived from Equation (2):

$$\beta k = \frac{C_T - \tau C_W}{C_F} - 1 \quad (4)$$

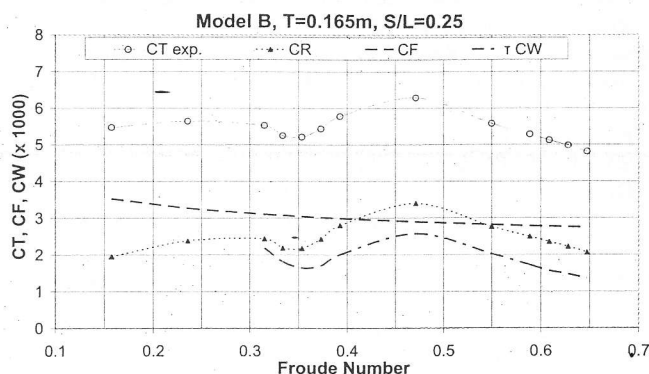


Figure 3. Results for Model B, $T=0.165$, trim=0, $S/L=0.25$

Table 3. Results for Model B, $T=0.165$, trim=0, $S/L=0.25$

V_m m/sec	Fn	C_T ($\times 10^3$)	C_R ($\times 10^3$)	C_F ($\times 10^3$)	τC_W ($\times 10^3$)	βk
2.459	0.393	5.781	2.795	2.986	2.000	0.266
2.951	0.471	6.285	3.391	2.893	2.570	0.284
3.443	0.550	5.578	2.760	2.819	2.024	0.261
3.689	0.589	5.283	2.496	2.786	1.720	0.279
3.812	0.609	5.119	2.348	2.771	1.563	0.283
3.934	0.628	4.975	2.219	2.757	1.470	0.272

As may be observed from Table 3, for the considered range of Froude numbers, the variation of βk is relatively small, ranging from 0.261 to 0.284 with an average value of 0.272. If this average value is used instead of the actual βk values in Equation (2), an approximation to C_T may be calculated.

The presented procedure has been applied for the calculation of the corresponding βk values for the various combinations of draughts, trims and separation distances, for the two models. Since our main interest is to establish a method for the evaluation of the bare hull, calm water resistance of high speed twin-hull vessels around the vicinity of their design speed, the average βk values have been calculated using only the experimental data corresponding to Froude numbers above 0.38. The obtained average βk values are summarized in Table 4 for Model A. The corresponding values for Model B are presented in Table 5.

A comparison of the experimentally measured C_T values and the numerical approximations using average βk values for the various combinations of draughts, trim and separation distances for Model A and Model B is presented in Figures 4 to 15. In the presented results, a very good agreement may be observed between the experimental C_T value and the numerical calculations for Froude numbers greater or equal to 0.40

Table 4. Calculated average βk values for Model A

S/L	T (m)	Trim (m)	βk
0.20	0.189	0.000	0.257
0.25	0.160	0.000	0.239
0.25	0.174	0.000	0.249
0.25	0.189	0.000	0.233
0.25	0.189	-0.017	0.211
0.30	0.189	0.000	0.264

Table 5. Calculated average βk values for Model B

S/L	T (m)	Trim (m)	βk
0.20	0.177	0.000	0.257
0.25	0.152	0.000	0.275
0.25	0.165	0.000	0.272
0.25	0.177	0.000	0.278
0.25	0.177	-0.017	0.280
0.30	0.177	0.000	0.262

This may be attributed to the accurate predictions of the C_W coefficient by SHIPFLOW and also to the relatively small variation of the βk coefficients in the considered range of Froude numbers, that justifies the use of average βk values. The obtained results for the wave interaction coefficient τ are presented in Figures 16-19. Figures 16 and 18 present the τ coefficient for Model A and B respectively, for a transverse spacing ratio $S/L=0.25$ and the three draughts corresponding to a length to volume ratio of 8.82, 9.135 and 9.50 for both models. Figure 17 presents the τ coefficient for Model A, at draught $T=0.189$ m ($L/V^{1/3}=8.82$) and for the three spacing ratios of $S/L=0.20$, 0.25 and 0.30. Figure 19 presents the τ coefficient for Model B, at draught $T=0.177$ m ($L/V^{1/3}=8.82$) and for the three spacing ratios of $S/L=0.20$, 0.25 and 0.30. Results are presented only for $Fn>0.3$, since for lower Froude numbers the calculations for the C_W coefficients were problematic. According to the presented results, τ becomes less than 1, indicating a favorable range of negative interactions between the wave systems of the two demi-hulls around $Fn=0.35$. For larger Froude numbers, τ increases considerably, obtaining its maximum values ranging from 1.28 to 1.45 at $Fn\approx 1.5$ as a result of strong positive interactions between the wave systems of the two demi-hulls.

Finally, the dynamic trim and the dynamic CG-rise, versus the ship speed, for the tested conditions are plotted in Figures 20 to 23. Positive angles correspond to bow up.

6 CONCLUSIONS

Results from a series of experiments along with the corresponding numerical calculations on the resistance prediction for two twin-hull models of the

semi-SWATH type have been presented and discussed. It has been confirmed that the employed numerical procedure can be used for a reliable resistance prediction, provided that an appropriate estimation of the form factor value is used. The development of a procedure for the estimation of the form factors, would be of great assistance to the designer, enabling the calculation of bare-hull calm water resistance of twin hull vessel, at least in the preliminary design stage. Further systematic work with various hull forms, in conjunction with the already published material by various researchers, would provide the basis for the establishment the above procedure.

ACKNOWLEDGMENTS

The authors wish to express their gratitude to Mr. Fotis Kassapis and Mr. Ioannis Trahanas for their valuable assistance in conducting the tank testing.

REFERENCES

Couser, P.R., Molland, A.F., Armstrong, N.A. and Utama, I.K.A.P. 1997. Calm Water Powering Predictions for High-Speed Catamarans. *Proc. Int. Conf. FAST '97, Sydney, Australia.*

Hughes, G. 1954. Friction and Form Resistance in Turbulent Flow, and a Proposed Formulation for Use in Model and Ship Correlation, *Transactions of the Institution of Naval Architects*, 94, 287.

Insel, M. and Molland, A.F. 1992. An Investigation into Resistance Components of High-Speed Displacement Catamarans. *Transactions of the Royal Institution of Naval Architects*, Vol. 134:1-20.

Larson, L. 1993. Resistance and Flow Predictions Using SHIPFLOW Code. *19th WEGEMT School, Nantes, France.*

Molland, A.F., Wellicome, J.F. and Couser, P.R. 1996. Resistance Experiments on a Systematic Series of High Speed Catamaran Forms: Variation of Length-Displacement Ratio and Breadth-Draught Ratio. *Transactions of the Royal Institution of Naval Architects*, Vol. 138.

Sahoo, P., Salas, M. and Schwetz, A. 2007. Practical Evaluation of Resistance of High-Speed Catamaran Hull-Forms – Part I. *Ships and Offshore Structures*, 2:4, 307-324.

Skoupas, S., Zaraphonitis, G. and Papanikolaou, A. 2009. Parametric Design and Optimization of High-Speed, Twin-Hull RoRo-Passenger Vessels. *Proc. Int. Marine Design Conf. IMDC '09, Trondheim, Norway.*

Zotti, L. 2005. Hydrodynamic experiments on a catamaran hull with a central bulb considering its resistance and seakeeping performances. *Maritime Transportation and Exploitation of Ocean and Coastal Resources*, Lisbon, Portugal..

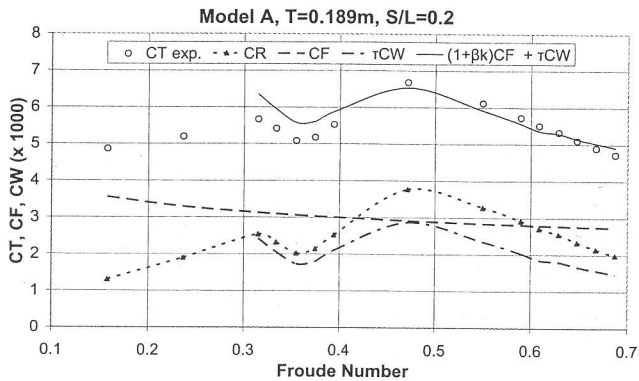


Figure 4. Resistance coefficients for Model A, $T=0.189\text{m}$, Trim=0m and $S/L=0.2$

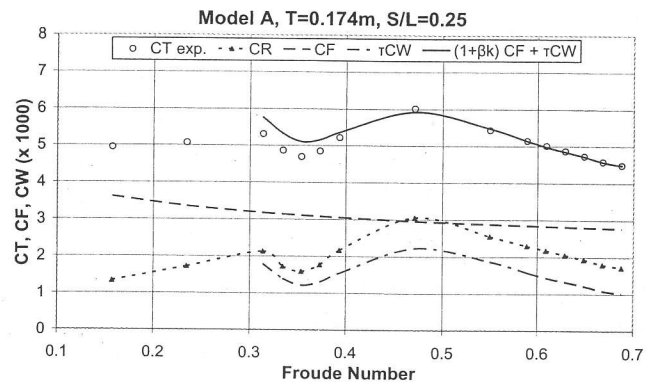


Figure 6. Resistance coefficients for Model A, $T=0.174\text{m}$, Trim=0m and $S/L=0.25$

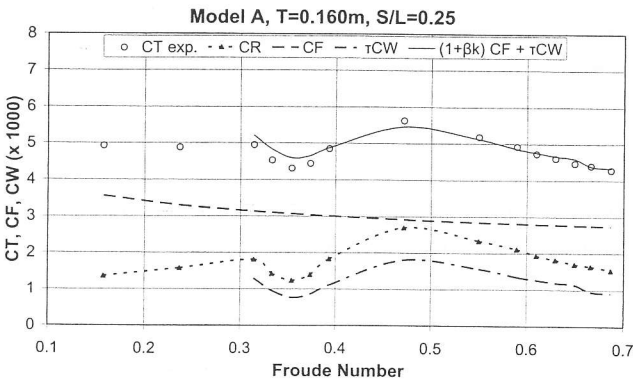


Figure 5. Resistance coefficients for Model A, $T=0.160\text{m}$, Trim=0m and $S/L=0.25$

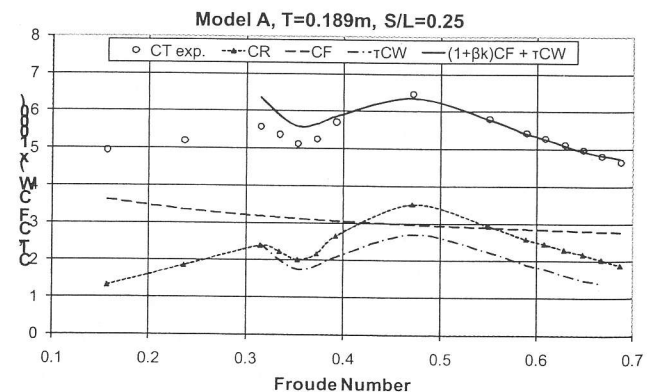


Figure 7. Resistance coefficients for Model A, $T=0.189\text{m}$, Trim=0m and $S/L=0.25$

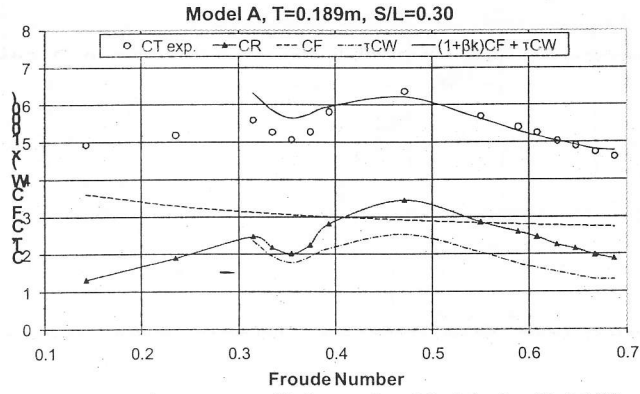


Figure 8. Resistance coefficients for Model A, $T=0.189\text{m}$, $\text{Trim}=0\text{m}$ and $S/L=0.30$

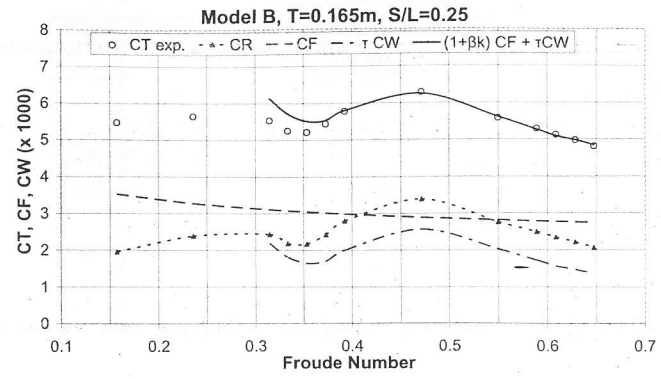


Figure 12. Resistance coefficients for Model B, $T=0.165\text{m}$, $\text{Trim}=0\text{m}$ and $S/L=0.25$

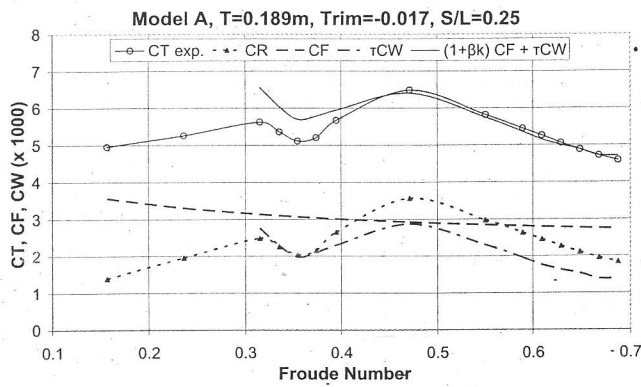


Figure 9. Resistance coefficients for Model A, $T=0.189\text{m}$, $\text{Trim}=-0.017\text{m}$ (by the stern) and $S/L=0.25$

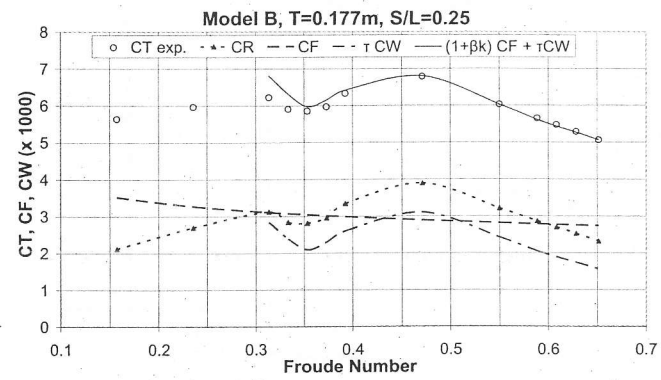


Figure 13. Resistance coefficients for Model B, $T=0.177\text{m}$, $\text{Trim}=0\text{m}$ and $S/L=0.25$

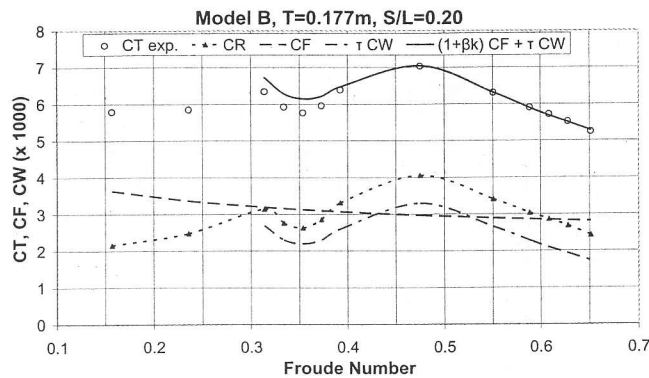


Figure 10. Resistance coefficients for Model B, $T=0.177\text{m}$, $\text{Trim}=0\text{m}$ and $S/L=0.2$

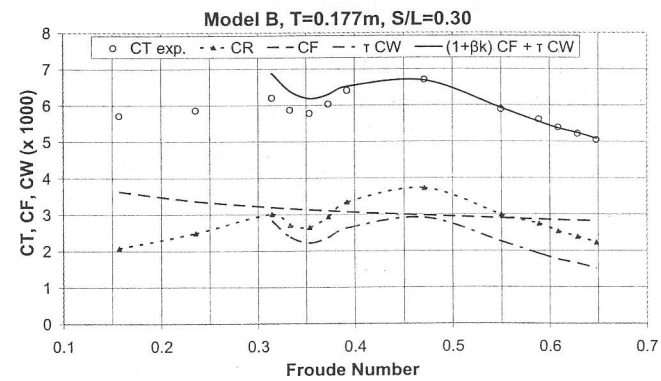


Figure 14. Resistance coefficients for Model B, $T=0.177\text{m}$, $\text{Trim}=0\text{m}$ and $S/L=0.30$

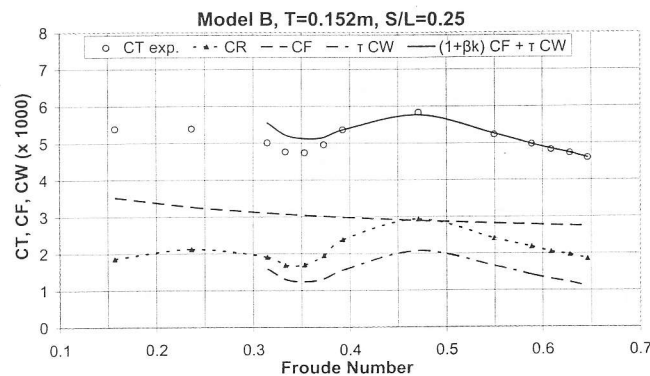


Figure 11. Resistance coefficients for Model B, $T=0.152\text{m}$, $\text{Trim}=0\text{m}$ and $S/L=0.25$

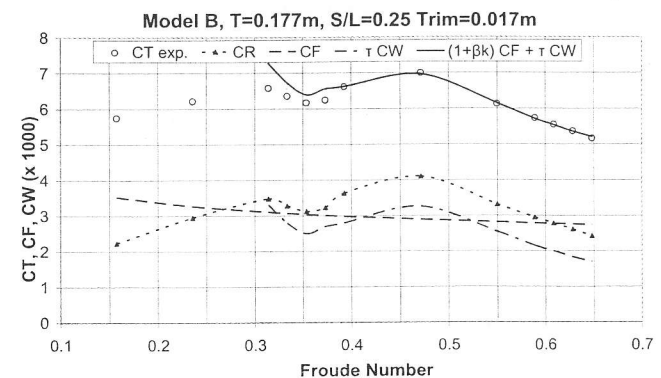


Figure 15. Resistance coefficients for Model B, $T=0.177\text{m}$, $\text{Trim}=-0.017\text{m}$ (by the stern) and $S/L=0.25$

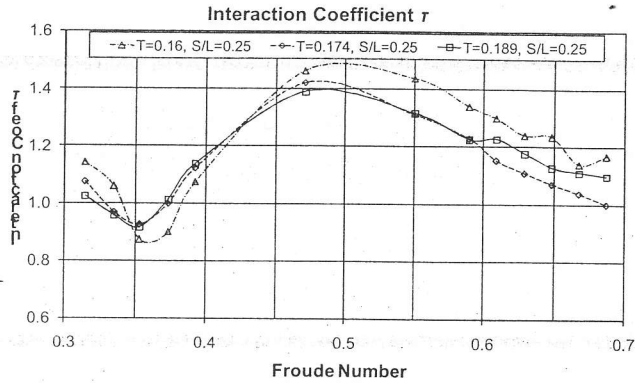


Figure 16. Wave interaction coefficients τ for Model A, $S/L=0.25$, Trim=0 and $L/\nabla^{1/3}=8.82, 9, 135$ and 9.50 .

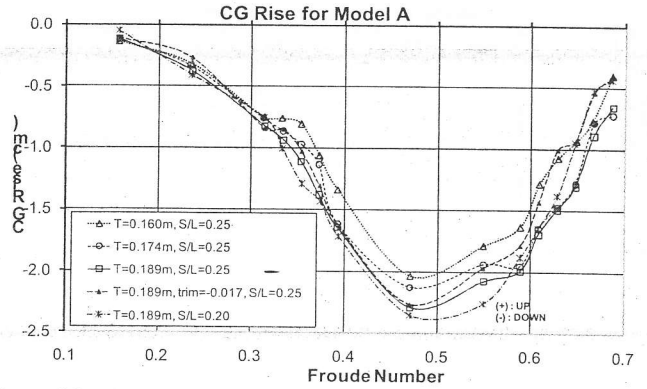


Figure 20. Measured CG Rise for Model A.

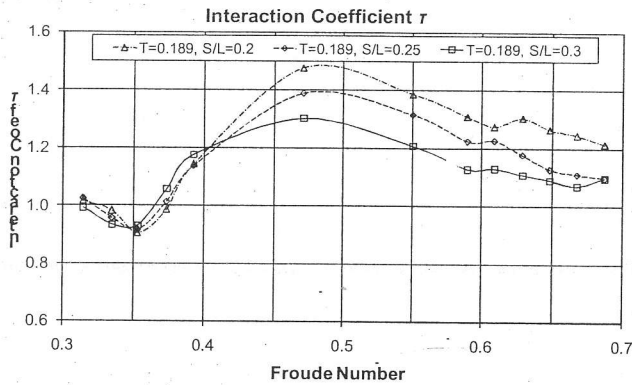


Figure 17. Wave interaction coefficients τ for Model A, $L/\nabla^{1/3}=8.82$ ($T=0.189m$), Trim=0 and $S/L=0.2, 0.25$ and 0.30 .

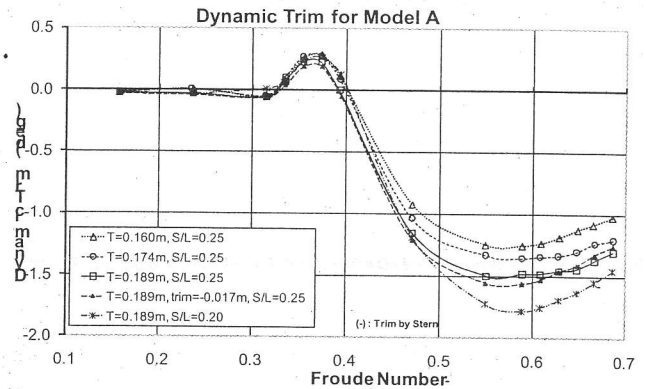


Figure 21. Measured Dynamic Trim for Model A.

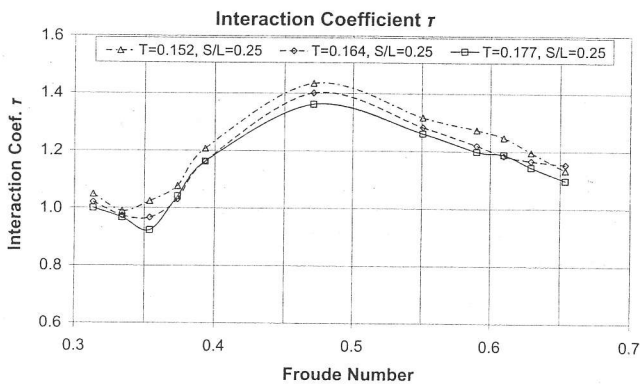


Figure 18. Wave interaction coefficients τ for Model B, $S/L=0.25$, Trim=0 and $L/\nabla^{1/3}=8.82, 9, 135$ and 9.50 .

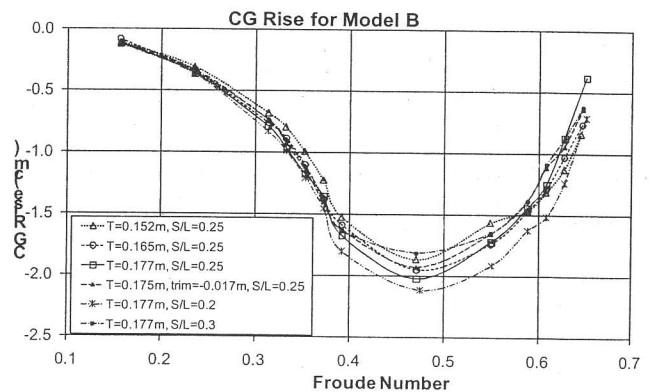


Figure 22. Measured CG Rise for Model B.

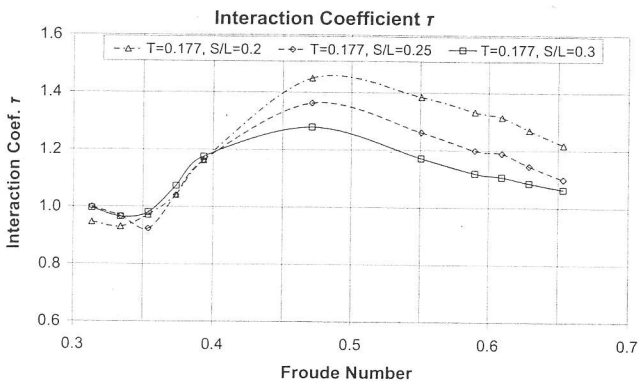


Figure 19. Wave interaction coefficients τ for Model B, $L/\nabla^{1/3}=8.82$ ($T=0.177m$), Trim=0 and $S/L=0.2, 0.25$ and 0.30 .

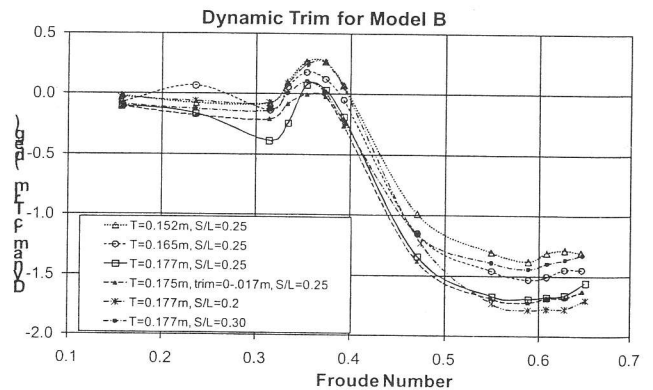


Figure 23. Measured Dynamic Trim for Model B.